NJC

Cite this: *New J. Chem.*, 2011, **35**, 476–482

www.rsc.org/njc

PAPER

3-Substituted xanthines as promising candidates for quadruplex formation: computational, synthetic and analytical studies†

János Szolomájer,[a] Gábor Paragi,[b] Gyula Batta,[c] Célia Fonseca Guerra,[d] F. Matthias Bickelhaupt,[d] Zoltán Kele,[a] Petra Pádár,[a] Zoltán Kupihár[a] and Lajos Kovács*[a]

Received (in Montpellier, France) 6th August 2010, Accepted 18th November 2010
DOI: 10.1039/c0nj00612b

Our computational studies suggest that 3-substituted xanthines are good candidates for tetrad and quadruplex structures. 3-Methylxanthine (3MX) has been synthesized from 7-benzylxanthine, and the existence of tetrameric and octameric aggregates of 3MX with NH_4^+, Na^+ and K^+ ions in the gas phase (MS) and in DMSO-d_6 solution (NMR) has been observed. The "internal" H-bonds (N1H···O6) are stronger than the "external" ones (N7H···O2) in these clusters (NMR).

Introduction

Molecules with a self-assembly ability are potential candidates for a wide range of applications from supramolecular chemistry to nanotechnology.[1] Guanine (G) tetrad structures are well known representatives of self-assembly in biological systems,[2] and the stacks of G-tetrads stabilized by cations (G-quadruplexes) play an important role in the regulation of cell proliferation by establishing the telomeric regions of DNA.[3] Quadruplexes, built up from at least two planar, stacking tetrad or tetramer units usually intercalated by cation(s), *e.g.* K^+, Na^+ NH_4^+, *etc.*, can also be the bottom line of the construction of supramolecular assemblies with designed optoelectronic properties.[4–6]

So far, several modifications have been suggested in the guanine motif, and the formed quadruplex structures have been experimentally examined.[7,8] Other purines (adenine,[9–12] hypoxanthine[8,13–16]) and pyrimidines (uracil,[17–19] thymine,[20] cytosine[21–23]) have also been investigated experimentally and computationally as building blocks of quadruplex structures. In all of these cases, the neighboring heterocycles are connected by only one H-bond in the tetrad structures, causing a weaker interaction and a less planar geometry than in guanine tetrads. Therefore, usually, an extra stabilizing interaction is required in the neighborhood of the tetrad, often exerted by sandwiching G-tetrads.

In the present paper, we propose 3-substituted xanthines as potential tetrad- and quadruplex-forming purine derivatives. The dominant 7*H* tautomeric form of a 3-substituted xanthine can bind to each neighboring xanthine moiety with two H-bonds in a tetrad, similarly to guanine. Therefore, we have anticipated that these assemblies should yield strong interactions and a planar geometry in the gas phase. As the simplest model, 3-methylxanthine (3MX) was chosen for our studies (Fig. 1) with or without additional cation.

Xanthine, its 9-glycosylated nucleosides, nucleotides and alkyl derivatives play a decisive role in a variety of intracellular metabolic pathways as substrates and/or intermediates of numerous enzymes or enzyme systems.[24] Xanthine, a substrate of both xanthine oxidase and xanthine dehydrogenase, is an intermediate in the formation of uric acid, the end product of purine nucleotide catabolism. The initial methyl acceptor from

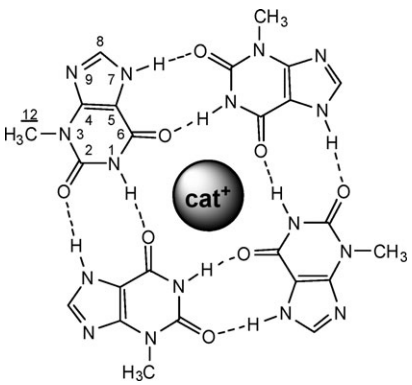

Fig. 1 Tetrads composed of 7*H*-3-methylxanthine (3MX) and different cations [cat^+ = none, Na^+, K^+, NH_4^+; purine atom and spectroscopic (underlined) numbering shown in upper left ring].

[a] *Department of Medicinal Chemistry, University of Szeged, Szeged, Hungary. E-mail: kovacs@ovrisc.mdche.u-szeged.hu; Fax: +36 62 545141; Tel: +36 62 545145*
[b] *Supramolecular and Nanostructured Materials Research Group of the Hungarian Academy of Sciences, University of Szeged, Szeged, Hungary*
[c] *Department of Organic Chemistry, University of Debrecen, Debrecen, Hungary*
[d] *Department of Theoretical Chemistry and Amsterdam Center for Multiscale Modeling (ACMM), Scheikundig Laboratorium der Vrije Universteit, Amsterdam, The Netherlands*
† Electronic supplementary information (ESI) available. See DOI: 10.1039/c0nj00612b

S-adenosylmethionine (SAM) for caffeine biosynthesis in tea and coffee plants is xanthosine (Xao) and/or xanthosine-5′-phosphate (XMP). XMP is an intermediate in the formation of guanosine-5′-monophosphate from inosine-5′-monophosphate (IMP) by IMP dehydrogenase. XTP is as efficient a phosphate donor as ATP for human deoxycytidine kinase.[24] 3MX possesses a bronchodilator effect,[25] it is an intermediate in the metabolism of methylxanthine alkaloids (caffeine, theophylline, theobromine)[26] and it also occurs in the marine invertebrate *Symplegma rubra*.[27] 3MX has recently been employed to study the dynamics of theophylline-binding RNA aptamers.[28,29] However, the properties of 3-substituted xanthine derivatives in tetrads/quadruplexes have not been investigated so far.

We examine herewith the tetrad- and octad-forming capacity of a 3-substituted xanthine starting from theoretical studies prior to experimental realization and detection. Following the theoretical considerations, 3MX[27,30] has been synthesized and the formation of higher-ordered structures has been investigated in gas (nano-ESI-MS) and solution (NMR) phase experiments.

Results and discussion

Computational studies

First, computational investigations have been performed for 3MX, as the simplest representative of the family of 3-substituted xanthines, at the BLYP-D/TZ2P level of dispersion-corrected density functional theory using ADF[31–33] and QUILD[34,35] programs. The optimized tetrameric and octameric structures are presented in Fig. 2 in the absence (2a) and presence (2b–2d) of cations. The calculated hydrogen bond energy of the four 3MX monomer in the tetrad amounted to −66.1 kcal mol^{-1} (Table 1).

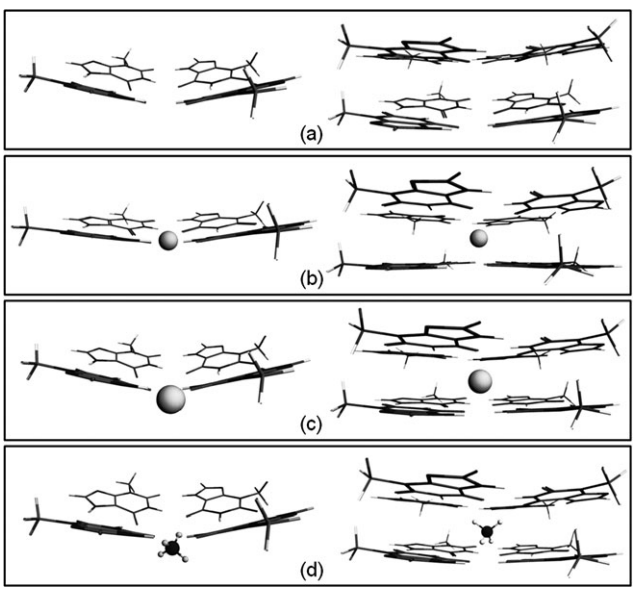

Fig. 2 Optimized tetrad (left panels) and octad structures (right panels) of 3MX without (a) and with cations ((b) Na^+, (c) K^+, (d) NH_4^+).

The optimized tetrad structures have been found to be bent, even in the ion-free case, but cations show a similar behavior to guanine tetrads.[8,23] Namely, the sodium ion tends to stay in the plane of the tetrad while potassium and ammonium ions occupy an out-of-plane position. According to the different ion radii of Na^+ (1.02 Å) and K^+ (1.38 Å), the results are reasonable and the similar out-of-plane optimums in the K^+ and NH_4^+ cases explain the ion bonding preference order in the gas phase. Thus, the stability order is $Na^+ > NH_4^+ \approx K^+$ and the binding energy values between the $(3MX)_4$ tetrad and the cations are −96.6, −71.8 and −70.3 kcal mol^{-1} for Na^+, NH_4^+ and K^+ ions, respectively.

Regarding the octads, the most planar structure was found with the sodium ion, and the structure without any intercalating ion had the most bent optimum. In all cases, the $(3MX)_4$ complex turned out to be more planar in the octad structure. Cations were found close to the midpoint between the layers, and the rotation of the two layers in the octads was *ca.* 17° in each aggregate. The distances between the layers have also been found to be very similar in each complex. Thus, neither the metallic ions nor the NH_4^+ affect the optimum stacking distance. Hydrogen bond distances d_n and bond angles α_n of tetrameric and octameric clusters have been defined and listed in Table 2. The "internal" H-bonds (N1H···O6) of the clusters are displayed with grey background, the "external" ones (N7H···O2) are shown in the area between the grey shadowing and the dashed grey circle. The "external" H-bonds are always very close to the ideal linear bond orientation in the slightly bent structures. These "external" bonds should be less linear in a planar geometry which can be also interpreted through the C═O and N–H bond angles α_n.

The orders of the strength of the ion-binding interaction in the octameric bilayer structure and the tetrad were the same ($Na^+ > NH_4^+ \approx K^+$). Note that the pure stacking bond energy between two $(3MX)_4$ tetrads is −47.0 kcal mol^{-1}. This is stronger than the corresponding stacking energy of the octameric 9-metylguanine cluster $(9MG)_8$ (−35.4 kcal mol^{-1}). Together with the theoretical results for tetrads, this prompted us to investigate the existence of $(3MX)_4$ and $(3MX)_8$ structures, with or without intercalating cations, experimentally.

Synthesis of 3-methylxanthine

3-Methylxanthine itself is commercially available. However, we wanted to elaborate a synthesis strategy that is generally applicable to the family of other 3-substituted xanthines as well. Therefore, the synthesis of 3-methylxanthine started with 7-benzylxanthine (**1**), available in two steps from guanosine according to the general method by Bridson *et al.*,[36] to obtain 3-substituted xanthines *via* an alkylation/deprotection scheme (Scheme 1). Methylation of the most acidic NH group (N3H) in the presence of K_2CO_3 resulted in the formation of 3-methyl (**2**) and 1,3-dimethyl (**3**)[37,38] derivatives in comparable quantities [for comparison, the pK_as for 7-methylxanthine are 8.35 (N3H) and *ca.* 13 (N1H)].[24] Reproducing the earlier method by Lister[39] to obtain 3MX using aq. NaOH for the methylation step raised the ratio of the monomethylated product and the conversion was higher. Bulkier substituents

Table 1 Components of ion binding energies (columns, in kcal mol^{-1}) of 3MX tetrads and octads (Na^+, K^+, NH_4^+ rows); the components of the formation energy of the tetrad and the stacking energy of the two tetrads are given in the 'none' rows. Values for tetrads are shown in bold

Cation	Cluster	$E_{interaction}$	$E_{deformation}$	$E_{binding}$
Na^+	**Tetrad + cation**	**−100.30**	**3.69**	**−96.61**
	Octad + cation	−135.78	10.56	−125.22
K^+	**Tetrad + cation**	**−73.09**	**2.75**	**−70.34**
	Octad + cation	−106.27	4.56	−101.71
NH_4^+	**Tetrad + cation**	**−75.58**	**3.75**	**−71.83**
	Octad + cation	−103.20	4.39	−98.81
None	**Four monomers**	**−73.62**	**7.52**	**−66.10**
	$Tetrad_1$ + $tetrad_2$	−51.84	4.80	−47.04

have been reported to give smaller amounts of by-products.[36] The debenzylation of **2** was rather challenging; the usual conditions of hydrogenation failed to give 3MX. The application of Pearlman's catalyst [$Pd(OH)_2$/C] in an amount far larger than catalytic at high pressure, elevated temperature and prolonged reaction time eventually furnished 3-methylxanthine. Alternatively, this deprotection could be achieved in an H-Cube® flow reactor, as well in a much shorter reaction time, with a smaller amount of catalyst, an easier work-up and in a higher yield.

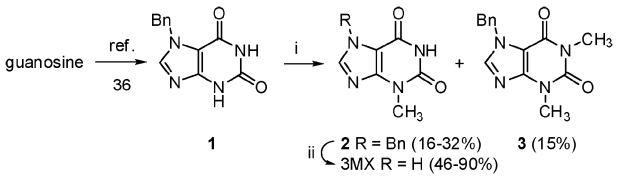

Scheme 1 (i) (A) K_2CO_3, CH_3I, anhydr. DMF, 50 °C, 16 h or (B) aq. NaOH, CH_3I, rt, 2 h, shaking; (ii) (A) H_2, $Pd(OH)_2$/C, 1,4-dioxane or AcOH, 90 °C, 75–100 bar, 24 h, batch reactor or (B) H_2, $Pd(OH)_2$/C, AcOH–EtOAc, 90 °C, 100 bar, H-Cube®, 25 min.

Mass spectrometric results

The tetrad formation of 3MX was first examined experimentally by mass spectrometry using a Q-TOF instrument equipped with a nano-ESI ion source. Although only NH_4^+ was intentionally added as an adduct-forming ion in aq. methanol, the most intense peak series in the mass spectrum (Fig. 3) contains Na^+, possibly due to an ion-exchange on the surface of the borosilicate capillary. This is in good accordance with the calculations, where the sodium ion is bound most strongly to the tetrad. Interestingly, the peak intensities increased along the series of adduct ions of $[3MX + Na]^+$, $[(3MX)_2 + Na]^+$, $[(3MX)_3 + Na]^+$ and $[(3MX)_4 + Na]^+$, in contrast to the "normal" case for compounds not forming tetrads.

Table 2 Hydrogen bond distances d_n (in Å) between the proton and the heteroatom along with the angles α_n (in degrees) of the pertinent H-bonds in 3MX clusters[a]

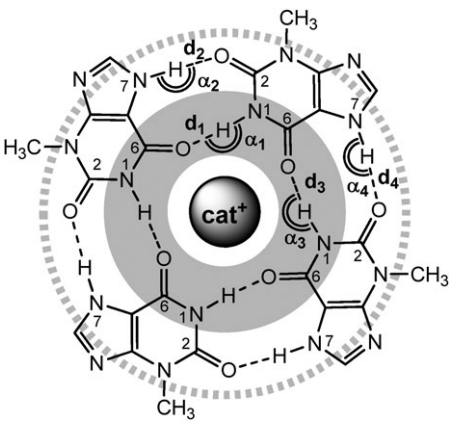

	Clusters	Symmetry (tetrad layer)		d_1 (d_3)	α_1 (α_3)	d_2 (d_4)	α_2 (α_4)
Tetramers	$(3MX)_4$	C_4	—	**1.73**	**170**	1.74	175
	$(3MX)_4 + Na^+$	C_4	—	**1.75**	**165**	1.77	176
	$(3MX)_4 + K^+$	C_4	—	**1.79**	**168**	1.75	173
	$(3MX)_4 + NH_4^+$	C_2	—	**1.76 (1.82)**	**170 (167)**	1.75 (1.78)	172 (175)
Octamers	$(3MX)_8$	C_4	(upper)	**1.70**	**169**	1.78	173
			(*lower*)	***1.70***	***171***	*1.77*	*174*
	$(3MX)_8 + Na^+$	C_4	(upper)	**1.70**	**164**	1.75	178
			(*lower*)	***1.71***	***163***	*1.75*	*178*
	$(3MX)_8 + K^+$	C_4	(upper)	**1.72**	**167**	1.80	176
			(*lower*)	***1.72***	***167***	*1.81*	*176*
	$(3MX)_8 + NH_4^+$	C_2	(upper)	**1.71 (1.74)**	**167 (168)**	1.81 (1.81)	175 (176)
			(*lower*)	***1.72 (1.71)***	***167 (169)***	*1.82 (1.81)*	*175 (175)*

[a] The "internal" H-bonds (N1H···O6) in the structure are displayed in bold (and also the corresponding values in the Table), the "external" ones (N7H···O2) are shown in the area between the grey shadowing and the dashed grey circle. In contrast to the C_2 symmetry case ($cat^+ = NH_4^+$), for C_4 symmetry clusters (cat^+ = none, Na^+, K^+), $d_1 = d_3$ ("internal" H-bonds, N1H···O6) and $d_2 = d_4$ ("external" H-bonds, N7H···O2). In the octads, these distances and angles slightly differ in the upper and *lower* tetrad layers.

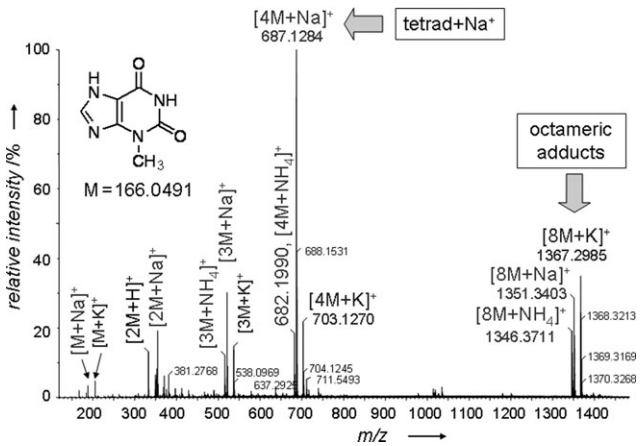

Fig. 3 Nano-ESI-Q-TOF MS spectrum of 3MX.

Furthermore, beyond the $[(3MX)_4 + Na]^+$ peak, the next most intense peak series in the upper mass region belongs to the $[(3MX)_8 + cat]^+$ peaks, suggesting an increased stability of the tetrad constructed by four 3MX molecules. These results are in line with the findings of Mezzache *et al.* on metal ion adducts of the parent xanthine.[8] In the region *m*/*z* 1012–1041, signals of very low intensity (1–4%) could also be observed that correspond to $[(3MX)_{12} + 2Na]^{2+}$ and $[(3MX)_{12} + Na + K]^{2+}$ beyond the $[(3MX)_6 + NH_4]^+$, (potentially $[(3MX)_6 + Na]^+$) and $[(3MX)_6 + K]^+$ clusters (data not shown).

Multinuclear NMR studies

Full ^1H, ^{13}C and ^{15}N NMR assignment of 3MX has been accomplished using standard HMBC techniques in DMSO-d_6 solution (~5 mg/500 μL) at 300 K (Table 3 and Table 4). These data support the tautomeric form shown in Fig. 1. Since the MS study suggests $(3MX)_n{\cdot}cat^+$ aggregates (n = 4, 8; $cat^+ = NH_4^+, Na^+, K^+$), several additional NMR experiments were carried out to disclose these features. Diffusion ordered spectroscopy (DOSY)[40–42] was used to determine the apparent molecular mass of the aggregates in solution. As an internal mass reference, tetramethylsilane was used because of its inertness and spherical structure.[43,44] As an apparent MW, 920 Da was obtained in DMSO-d_6 solution at 300 K. For a $(3MX)_4$ aggregate, MW = 664 Da is expected, and the difference between the experimental and theoretical values may be attributed to solvent molecules associated with the clusters of 3MX. When 0.4 equiv. of potassium picrate was added to the solution, the apparent MW increased to 1130 Da. Further increasing the potassium picrate concentration to 1.04 equiv. did increase the apparent MW up to 1300 Da. On the contrary, increasing the temperature to 315 K decreased the apparent MW to 710 Da. It should be noted that DOSY may have a 10–15% error for the apparent MW, as estimated from repeated experiments. In other solvents (water, DMF, methanol, chloroform), the solubility was generally poor. We did not observe association *e.g.* in dilute water–DMSO solution [ε = 78.4 (water), ε = 46.45 (DMSO)]. This is in accordance with the observation that co-solvents or co-solutes with relatively low dielectric constants are known to stabilize quadruplexes.[45]

To observe the intermolecular H-bonding in the self-assemblies, we measured the deuteration isotope shifts[46] on the acceptor carbonyls, but this was not indicative because of the concurrent two- and three-bond intramolecular effects. Similarly, NH proton chemical shift temperature dependencies were not well above the accepted limits for H-bonding (N7H = −4.5 ppb K^{-1}, N1H = −6.1 ppb K^{-1}). In selective transient 1D NOESY experiments,[47] we observed significant magnetization transfer between N7H and water due to exchange, while in the case of N1H, this transfer was negligible. Consequently, we suppose that the "internal" H-bonds (N1H···O6) in the $(3MX)_4$ structures must be stronger than the "external" H-bonds (N7H···O2). This was also the case for the gas phase theoretical results, according to which the "internal" H-bonds have always been shorter than the "external" ones (Table 2). Ribbon-like structures in solution of indefinite MW would involve equally both N1H and NH7, and therefore can be excluded as the two protons behave very differently (see above). Concerning the homonuclear NOEs from the same 1D NOESY experiments, only a small NOE is seen between the N1H and $N3CH_3$ group, and a stronger intramolecular effect between N7H and C8H can be observed. Intermolecular effects of N7H may possibly be reduced by water exchange and were not observed. Using steady state $^{13}C\{^1H\}$ heteronuclear NOE,[48,49] we observed 14 and 44% heteronuclear NOE at C6 and C2, respectively, when N1H was saturated, while these carbons were "silent" when N7H was

Table 3 NMR data of 3MX[a]

Atom no.[b]	Group	Estimated ^{13}C chemical shift[c] (ppm)	^{13}C (exp.)/ppm	^1H (exp.)/ppm	^{15}N (exp.)/ppm	^{13}C deuteration isotope shift/ppb
2	C	151.2	151.05	—	—	−87
4	C	149.4	149.56	—	—	0
5	C	106.9	106.69	—	—	−150
6	C	154.7	154.05	—	—	−36
8	CH	140.5	140.42	8.008	—	0
12	CH_3	28.8	28.62	3.371	—	0
1	NH	—	—	11.074	153.35	—
7	NH	—	—	13.480	159.89	—
9	N	—	—	—	234.45	—
3	N	—	—	—	112.86	

[a] DMSO-d_6 solution, T = 300 K, reference: TMS = 0 ppm, 5 mg 3-methylxanthine in 500 μL DMSO-d_6 + *ca.* 5 equiv. H_2O. Non-trivial ^{13}C HMBC: $^4J_{H8,C6}$. [b] For numbering, see Fig. 1. [c] ACD/NMR predictor.

Table 4 ^{15}N–^{1}H couplings in 3MX from ^{15}N-HMBC experiments

Coupling/Hz	Assignment
7.6	$^{2}J_{H8,N7}$
12	$^{2}J_{H8,N9}$
<4	$^{3}J_{H1,N3}$
<4	$^{2}J_{H3C,N3}$
90.5	$^{1}J_{1NH,N}$

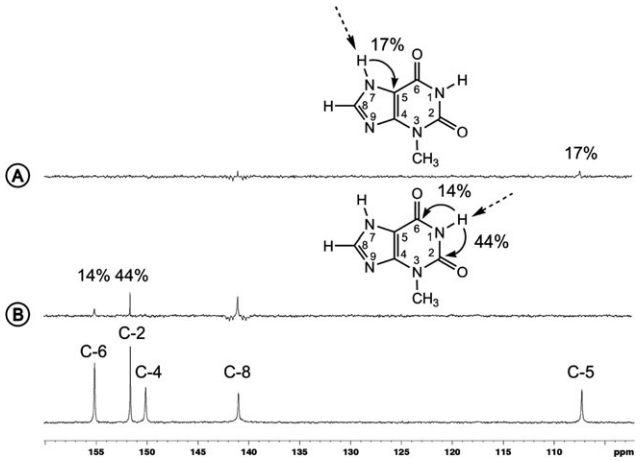

Fig. 4 Steady state $^{13}C\{^{1}H\}$ heteronuclear NOE[48,49] data of 3MX. N7H (trace A) and N1H irradiation (trace B).

irradiated, though at C-5 the two-bond hetero NOE yielded a 17% enhancement (Fig. 4). Furthermore, no couplings *via* intermolecular H-bonds were detected in either ^{15}N or ^{13}C HMBC experiments. In summary, the DOSY experiments seem to support the presence of $(3MX)_4{\cdot}cat^+$ and possibly $(3MX)_8{\cdot}cat^+$ (cat^+ = none or K^+) clusters in DMSO-d_6 solution, but it is difficult to prove unequivocally the H-bond pattern by direct NMR methods, most likely because of the dynamic nature of the weak self-assemblies.

Conclusions

Our gas-phase computational studies suggest that 3MX is a good candidate for tetrad and quadruplex structures. 3MX has been synthesized, and the existence of $(3MX)_4{\cdot}cat^+$ and $(3MX)_8{\cdot}cat^+$ ($cat^+ = NH_4^+, Na^+, K^+$) aggregates in the gas phase has been indeed observed (MS). Detailed NMR studies have also verified that the "internal" H-bonds (N1H···O6) in the $(3MX)_4$ structures must be stronger than the "external" H-bonds (N7H···O2). Clearly, to achieve stronger interactions in tetrads/quadruplexes composed of 3-substituted xanthines, substituents in position 3 other than methyl should be present to allow for further stabilization, and this work is in progress. Additionally, 3-substituted xanthines also have the potential to form base pairs with DNA or RNA in a Watson–Crick and/or Hoogsteen manner.

Experimental

Computational methods

The calculations were performed at the BLYP-D/TZ2P level of theory in each case, and the final geometry was determined with 10^{-5} and 10^{-6} accuracy for the gradient and energy, respectively. C_4 symmetry was applied for all systems, except for complexes with a NH_4^+ ion which have C_2 symmetry. The definition of binding energy is $E_{binding} = E_{interaction} + E_{deformation}$, where $E_{interaction}$ is equal to the total energy of the complex minus the sum of the total energy of the independent fragments. $E_{deformation}$ is the amount of energy required to deform the separate fragments from their equilibrium structure to the geometry that they acquire as a complex. A detailed introduction to the calculation of interaction energy ($E_{interaction}$) can be found in a paper by Bickelhaupt and Baerends.[50]

Synthesis

Unless otherwise noted, solvents and reagents were of reagent grade from commercial suppliers and used without further purification. Pearlman's catalyst refers to $Pd(OH)_2/C$ with 20% Pd content, Alfa Aesar cat. no. 042578. All moisture-sensitive reactions were performed under an argon atmosphere using oven-dried glassware. The H-Cube® reactor was the product of ThalesNano, Budapest, Hungary (http://www.thalesnano.com/products/h-cube). Reactions were monitored by TLC on Kieselgel 60 F_{254} plates (Merck) with detection by UV. Flash column chromatography was carried out using silica gel (particle size 40–63 μm). Melting points are uncorrected. Elementary analyses: Perkin-Elmer CHN analyzer model 2400. Low resolution ESI-MS spectra were obtained on a Finnigan MAT TSQ 7000 instrument. ^{1}H, ^{13}C and ^{15}N NMR spectra were recorded in DMSO-d_6 using Bruker Avance DRX 500 instruments. J values are given in Hz.

Methylation of 7-benzylxanthine (2)

Method A[36]. Compound **1**[36] (0.900 g, 3.72 mmol) was dissolved in anhydrous DMF (20 mL) under sonication. K_2CO_3 was added (0.616 g, 4.46 mmol, 1.2 equiv.) and the heterogeneous solution heated with vigorous stirring at 50 °C for 1 h. The obtained potassium salt was treated dropwise with methyl iodide (0.527 g, 3.72 mmol, 1.0 equiv.) in anhydrous DMF (20 mL) and the reaction mixture stirred at 50 °C for 16 h. The heterogeneous solution was filtered, the filtrate evaporated *in vacuo* and co-evaporated with EtOH (2×) and CH_3CN (2×). The residue was dissolved in EtOAc (500 mL) and extracted with H_2O (5×100 mL). The organic layer was dried (Na_2SO_4), filtered and evaporated *in vacuo*. The crude product was purified by column chromatography using the solvent system 5–20 v/v% EtOAc in CH_2Cl_2 to give compounds **2** (155 mg, 16.3%) and **3** (150 mg, 14.9%), along with unreacted starting material **1** (0.619 g, 68.8%).

7-Benzyl-3-methylxanthine (2)[39]. mp.: 274.2–277.2 °C (lit. 272–275 °C).[39] ESI-MS (m/z): 256.65 (100, $[M + H]^+$). The ^{1}H NMR data were in accordance with the published values.[39] Elemental analysis calc. (%) for $C_{13}H_{12}N_4O_2$ (256.260): C, 60.93; H, 4.72; N, 21.86; found C, 60.81; H, 4.83; N, 21.62.

7-Benzyl-1,3-dimethylxanthine (3)[37,38]. mp.: 158.2–159.2 °C (lit. 158.6–159.4 °C).[37,38] The ^{1}H and ^{13}C NMR data were in accordance with the published values.[37–39] ESI-MS

(m/z): 270.66 (100, $[M + H]^+$). Elemental analysis calc. (%) for $C_{14}H_{14}N_4O_2$ (270.287): C, 62.21; H, 5.22; N, 20.73; found C, 62.40; H, 5.38; N, 20.62.

Method B[39]. Compound **1**[36] (0.900 g, 3.72 mmol) was dissolved in water (12 mL) and 1 M sodium hydroxide (4.5 mL, 1.2 equiv.) under sonication and warmed to effect dissolution. After the addition of methyl iodide (0.527 g, 3.72 mmol, 1 equiv.), the reaction mixture was shaken for 2 h using a peptide shaker. The obtained heterogeneous solution was diluted with water (500 mL) and extracted with EtOAc (5 × 100 mL). The organic layer was dried (Na_2SO_4), filtered, evaporated *in vacuo* and co-evaporated with MeCN (3 × 100 mL). The crude product was purified by column chromatography using the solvent system 5–20 v/v% EtOAc in CH_2Cl_2 to give compounds **2** (0.300 g, 31.5%) and **3** (0.148 g, 14.7%), along with unreacted starting material **1** (0.483 g, 53.8%).

3-Methylxanthine (3MX)[27,30]

Method A. Compound **2** (500 mg, 1.95 mmol) was dissolved in 1,4-dioxane or AcOH (50 mL) and Pearlman's catalyst (0.96 g) was added in a batch reactor. The reactor was filled with H_2 (75–100 bar) and the reaction mixture heated at 90 °C with stirring for 24 h. The reaction mixture was filtered, the filtrate evaporated *in vacuo* and co-evaporated with MeCN (3×). The crude product was purified by column chromatography using the solvent system 20 v/v% MeOH in CH_2Cl_2 to give the product (150 mg, 46.3%). 3MX was crystallized from water. Mp. > 300 °C. ESI-MS (m/z): 167 ($[M + H]^+$). Elemental analysis calc. (%) for $C_6H_6N_4O_2$ (166.137): C, 43.38; H, 3.64; N, 33.72; found C, 43.51; H, 3.50; N, 33.93. For detailed NMR data, see Table 3, Table 4 and Fig. 4.

Method B. Compound **2** (25 mg, 0.0975 mmol) was dissolved in 15 v/v% AcOH in EtOAc (25 mL). A cartridge for the H-Cube® reactor was loaded with Pearlman's catalyst (20 mg). The catalyst was activated for 15 min in a H_2 atmosphere (100 bar). Debenzylation in the H-Cube® flow reactor was conducted at 90 °C, a 100 bar H_2 atmosphere and at a 1 mL min^{-1} flow rate for 25 min. The catalyst could be reused several times. The solution was evaporated and the product (3MX) recrystallized from water (14.5 mg, 90%). The analytical data (R_f, ^1H, ^{13}C NMR, MS) of this sample were identical with that obtained using *Method A*.

Nano-ESI-MS data of 3-methylxanthine (3MX) aggregates

High resolution mass spectrometry experiments were performed on a Waters MALDI Q-TOF Premier instrument equipped with a nano-ESI ion source containing a gold-coated borosilicate capillary tip. Voltages: capillary: 1.4–1.8 kV, sampling cone: 28 V, extraction cone: 4.9 V; source temperature: 95 °C; cone gas 20 l h^{-1}; nanoflow gas: 0. The sample was prepared in the following way: a saturated aqueous solution of 3-MX, containing 100 mM NH_4HCO_3 (pH 8) and methanol saturated with NH_4HCO_3 were mixed in a 1 : 99 ratio, and the resulting dilute solution was used directly for experiments.

NMR data of 3-methylxanthine (3MX) aggregates

See Table 3, Table 4 and Fig. 4.

Acknowledgements

This study was supported by grants OTKA NK 73672, NK 68578, CK 77515, COST Action MP0802, TÁMOP 4.2.1.B 09/1/KONV, University of Szeged, HPC-Europa2, Free University of Amsterdam and the SARA Supercomputing Center. We also thank the Netherlands Organization for Scientific Research (NWO-CW and NWO-NCF) and the National Research School Combination-Catalysis (NRSC-C) for financial support, and Mr. István Mándity for his assistance with the H-Cube® flow reactor.

Notes and references

1 J. W. Steed and J. L. Atwood, *Supramolecular Chemistry*, John Wiley and Sons, Chichester, 2000.
2 S. Neidle and S. Balasubramanian, *Quadruplex Nucleic Acids*, The Royal Society of Chemistry, Cambridge, 2006.
3 S. Neidle, *FEBS J.*, 2009, **277**, 1118–1125.
4 J. T. Davis and G. P. Spada, *Chem. Soc. Rev.*, 2007, **36**, 296–313.
5 S. Lena, S. Masiero, S. Pieraccini and G. P. Spada, *Chem.–Eur. J.*, 2009, **15**, 7792–7806.
6 M. Franceschin, *Eur. J. Org. Chem.*, 2009, 2225–2238.
7 J. Gros, F. Rosu, S. Amrane, A. De Cian, V. Gabelica, L. Lacroix and J.-L. Mergny, *Nucleic Acids Res.*, 2007, **35**, 3064–3075.
8 S. Mezzache, S. Alves, J. P. Paumard, C. Pepe and J. C. Tabet, *Rapid Commun. Mass Spectrom.*, 2007, **21**, 1075–1082.
9 P. K. Patel, A. S. R. Koti and R. V. Hosur, *Nucleic Acids Res.*, 1999, **27**, 3836–3843.
10 B. C. Pan, Y. Xiong, K. Shi, J. P. Deng and M. Sundaralingam, *Structure*, 2003, **11**, 815–823.
11 T. van der Wijst, B. Lippert, M. Swart, C. Fonseca Guerra and F. M. Bickelhaupt, *JBIC, J. Biol. Inorg. Chem.*, 2010, **15**, 387–397.
12 C. Fonseca Guerra, T. van der Wijst, J. Poater, M. Swart and F. M. Bickelhaupt, *Theor. Chem. Acc.*, 2010, **125**, 245–252.
13 F. W. Smith and J. Feigon, *Biochemistry*, 1993, **32**, 8682–8692.
14 F. W. Smith, P. Schultze and J. Feigon, *Structure*, 1995, **3**, 997–1008.
15 B. C. Pan, K. Shi and M. Sundaralingam, *J. Mol. Biol.*, 2006, **363**, 451–459.
16 F. C. Meng and X. Zhao, *THEOCHEM*, 2008, **869**, 94–97.
17 C. J. Cheong and P. B. Moore, *Biochemistry*, 1992, **31**, 8406–8414.
18 E. L. Zins, S. Rochut and C. Pepe, *J. Mass Spectrom.*, 2009, **44**, 813–820.
19 E. L. Zins, S. Rochut and C. Pepe, *J. Mass Spectrom.*, 2009, **44**, 40–49.
20 P. K. Patel and R. V. Hosur, *Nucleic Acids Res.*, 1999, **27**, 2457–2464.
21 P. K. Patel, N. S. Bhavesh and R. V. Hosur, *Biochem. Biophys. Res. Commun.*, 2000, **270**, 967–971.
22 J. Šponer and N. Špačková, *Methods*, 2007, **43**, 278–290.
23 J. D. Gu and J. Leszczynski, *Chem. Phys. Lett.*, 2002, **351**, 403–409.
24 E. Kulikowska, B. Kierdaszuk and D. Shugar, *Acta Biochim. Polon.*, 2004, **51**, 493–531.
25 J. Song, K. U. Park, H. D. Park, Y. Yoon and J. Q. Kim, *Clin. Chem.*, 2004, **50**, 2176–2179.
26 Caffeine metabolism. KEGG map 00232, 2009 (http://www.genome.jp/kegg/pathway/map/map00232.html).
27 B. S. Lindsay, A. M. P. Almeida, C. J. Smith, R. G. S. Berlinck, R. M. da Rocha and C. M. Ireland, *J. Nat. Prod.*, 1999, **62**, 1573–1575.
28 G. A. Soukup, G. A. M. Emilsson and R. R. Breaker, *J. Mol. Biol.*, 2000, **298**, 623–632.
29 S. W. Lee, L. Zhao, A. Pardi and T. B. Xia, *Biochemistry*, 2010, **49**, 2943–2951.

30 K. Lafleur, D. Z. Huang, T. Zhou, A. Caflisch and C. Nevado, *J. Med. Chem.*, 2009, **52**, 6433–6446.
31 E. J. Baerends, *et al.*, ADF2009.01, *Scientific Computing and Modeling (SCM)*, Department of Theoretical Chemistry, Vrije Universiteit, Amsterdam, The Netherlands, 2009 (http://www.scm.com).
32 G. T. te Velde, F. M. Bickelhaupt, E. J. Baerends, C. Fonseca Guerra, S. J. A. van Gisbergen, J. G. Snijders and T. Ziegler, *J. Comput. Chem.*, 2001, **22**, 931–967.
33 C. Fonseca Guerra, J. G. Snijders, G. te Velde and E. J. Baerends, *Theor. Chem. Acc.*, 1998, **99**, 391–403.
34 M. Swart and F. M. Bickelhaupt, *Int. J. Quantum Chem.*, 2006, **106**, 2536–2544.
35 M. Swart and F. M. Bickelhaupt, *J. Comput. Chem.*, 2008, **29**, 724–734.
36 P. K. Bridson, G. Richmond and F. Yeh, *Synth. Commun.*, 1990, **20**, 2459–2467.
37 M. N. S. Rad, A. Khalafi-Nezhad, S. Behrouz, M. A. Faghihi, A. Zare and A. Parhami, *Tetrahedron*, 2008, **64**, 1778–1785.
38 M. N. S. Rad, A. Khalafi-Nezhad, S. Behrouz, Z. Asrari, M. Behrouz and Z. Amini, *Synthesis*, 2009, 3067–3076.
39 J. H. Lister, *Aust. J. Chem.*, 1979, **32**, 387–397.
40 C. S. Johnson, *Prog. Nucl. Magn. Reson. Spectrosc.*, 1999, **34**, 203–256.
41 D. H. Wu, A. D. Chen and C. S. Johnson, *J. Magn. Reson., Ser. A*, 1995, **115**, 260–264.
42 G. A. Morris and H. Barjat, in *Methods for Structure Elucidation by High-Resolution NMR*, ed. G. Batta, K. E. Kövér and C. Szántay Jr., Elsevier, Amsterdam, 1997, pp. 209–226.
43 L. Orosz, G. Batta, S. Kéki, M. Nagy, G. Deák and M. Zsuga, *Carbohydr. Res.*, 2007, **342**, 1323–1328.
44 G. Pintér, G. Batta, P. Horváth, I. Löki, T. Kurtán, S. Antus, S. Kéki, M. Zsuga, G. Nagy, J. Aradi, T. Gunda and P. Herczegh, *Langmuir*, 2007, **23**, 5283–5285.
45 I. V. Smirnov and R. H. Shafer, *Biopolymers*, 2007, **85**, 91–101.
46 T. Dziembowska, P. E. Hansen and Z. Rozwadowski, *Prog. Nucl. Magn. Reson. Spectrosc.*, 2004, **45**, 1–29.
47 K. Stott, J. Stonehouse, J. Keeler, T. L. Hwang and A. J. Shaka, *J. Am. Chem. Soc.*, 1995, **117**, 4199–4200.
48 K. E. Kövér and G. Batta, *Prog. Nucl. Magn. Reson. Spectrosc.*, 1987, **19**, 223–266.
49 H. B. Seba, P. Thureau, B. Ancian and A. Thevand, *Magn. Reson. Chem.*, 2006, **44**, 1109–1117.
50 F. M. Bickelhaupt and E. J. Baerends, *Rev. Comput. Chem.*, 2000, **15**, 1–86.

